Strain field of interstitial hydrogen atom in body-centered cubic iron and its effect on hydrogen-dislocation interaction

Shuai Wang[a,*], Keisuke Takahashi[a], Naoyuki Hashimoto[a], Shigehito Isobe[b], Somei Ohnuki[a]

[a] *Graduate School of Engineering, Hokkaido University, N-13, W-8, Sapporo 060-8278, Japan*
[b] *Creative Research Institution, Hokkaido University, N-21, W-10, Sapporo 001-0021, Japan*

Abstract

Effect of hydrogen in body-centered cubic iron is explored by using the density function theory. Hydrogen atoms increase the concentration of free electrons in the simulation cell and have bonding interaction with Fe atom. Caused by anisotropic strain components of hydrogen atoms in the tetrahedral sites, elastic interaction for hydrogen with screw dislocation has been found. The dependence of hydrogen-screw dislocation interaction on hydrogen concentration is confirmed by repeated stress relaxation tests.

Keywords: density function theory; hydrogen embrittlement; iron alloys; stress relaxation

The strain field of H in iron is of crucial importance in understanding the H-dislocation interactions. As a perfect screw dislocation only expresses shear stress field, the interstitial atoms which have components of strain

*Corresponding author TEL, FAX: +81-11-706-6772.
Email address: towangshuai@eng.hokudai.ac.jp (Shuai Wang)

tensor equivalent in three axis of a rectangular coordinate ($\epsilon_{11} = \epsilon_{22} = \epsilon_{33}$) only interact with edge type dislocations. The assumption of such simple dilatation field has been applied to H atoms in many reports [1], in particular, in the theoretical framework of hydrogen enhanced plasticity model (HELP) [2] which now becomes one of the most accepted theories for understanding hydrogen embrittlement. The hydrogen-induced Snoek type internal friction peak has been observed in both BCC and FCC iron [3, 4], it was suggested that such Snoek type peak could be caused by unequal strain components, e.g. $\epsilon_{11} \neq \epsilon_{22}$ [1] . However, due to the low solubility and fast diffusion of H atoms, there is no direct measurement that can support the results for the bulk metal, and argument still exists.

This study introduces the analysis of electron structure of H-BCC iron system and the strain field of H atom based on density functional theory (DFT). For the first time, we combine the DFT calculation results with the classical calculation method developed by Cochardt et al. [5], which evaluates the interaction of interstitial atom with dislocation and has been proved to be in good agreement with experimental results for C interstitial atoms in BCC iron. The interaction of H with both edge type and screw type dislocations will be discussed. Hydrogen effects on dislocation motion will also be discussed based on repeated transients tests.

The grid-based real-space code GPAW [6] was used for DFT calculations. It is an implementation of the projector augmented wave (PAW) method of Blöchl [7], which is an all-electron full-potential method within the frozen core approximation. The Atomic Simulation Environment (ASE) [8] provided an interface to GPAW. The Perdew-Burke-Ernzerhof (PBE) parametrization

was used for the approximation of the exchanged-correlation (xc) function [9]. Spin polarized calculation was performed with an initial magnetic moment of 2.20 for iron atoms. $(4 \times 4 \times 4)$ k points of the Brillouin zone sampling which uses the Monkhorst-Pack scheme was carried out [10, 11] with grid spacing of 0.18 Å and Fermi smearing of 0.1 eV.

Bulks of BCC iron with $(2 \times 2 \times 2)$ cell were created (Fe_{16}) and vacancy defect was imposed in some bulks (Fe_{15}). Periodic boundary conditions are considered for all calculations. H atoms were inserted initially into tetrahedral positions of the cell, for the experimental evidence indicated such hydrogen occupancy for BCC Fe [1]. The variations of electron charge by adding hydrogen were analyzed by a fast and robust algorithm implemented by Tang et. al [12] based on the Bader partitioning scheme [13]. All calculations were made for 0 K. The calculated lattice constant of Fe_{16} is 2.8369 Å, bulk modulus is 162 GPa and magnetic moment is 2.17 μ_B, which are in good accordance with the results from experiment (2.8665 Å, 165 $\pm$ 5 GPa, 2.22 μ_B) and other calculations [14].

Large H concentrations were used in our DFT calculations ($C_H > 6\%$), but hydrogen has much lower solubility at experimental conditions [1]. To investigate strain filed with C_H close to the experimental value, molecular dynamics (MD) calculation using embedded atom method (EAM) with the Potential B reported by Ramasubramaniam et al. [15] was carried out on a $Fe_{106561}H_1$ cell ($C_H < 10$ appm). LAMMPS code distributed by Sandia National Laboratories was used as MD simulator [16], and the relaxation of structure was performed by the conjugate gradient (CG) method.

The elastic interaction between H and dislocations was studied following

the classical method developed by Cochardt et al. [5]. In BCC iron the symmetry of both the octahedral site and tetrahedral site are expected to produce a strain field with local tetragonal symmetry. Since the exact atomic arrangement can be calculated using DFT method in this study, a strain tensor S_H of a unit cell containing one H atom can be obtained as $S_H = \{\epsilon_{11}, \epsilon_{22}, \epsilon_{33}\}$. If stress tensor $T_D = \sigma_{ij}^D$ of the dislocation field is expressed in the same coordinate system as the strain tensor S_H, the elastic interaction energy U_{DH} can be written as:

$$U_{DH} = -(T_D, S_H)a^3 = -\Sigma_{ij}\sigma_{ij}^D\epsilon_{ij}^H a^3 \tag{1}$$

where a is the lattice constant. For the strain tensor which are not in the same coordinate system with σ_{ij}^D, crystallographic relations is used for transforming the interstitial strain tensor into the same coordinate as the stress field of dislocations, for details can refer to the calculations focused on carbon atoms [5].

The repeated stress relaxation test developed by Spätig [17] has shown advantages in evaluating thermal activated behavior of dislocations, and such test was applied on hydrogen-charged iron specimens with purity better than 99.996%, and grain size of 75±10 μm. After cold rolling and punching, tensile specimen was annealed at 873 K in vacuum tube (1×10^{-4} Pa). The electrolyte for hydrogen charging is 0.5mol/l H_2SO_4 adding 50g/l Thiourea (promoter) and hydrogen charging was sustained in all relaxations. At 293 K, the samples were initially strained with strain rate of 1×10^{-4} s^{-1} to 5% after the yield point. In each relaxation the tensile cross-head was stopped for 30 s and the strain is constant. Thermal activation analysis was based

on the obtained decreased stress ($\Delta\tau$) v.s. time (t) curves. The effective activation volume for dislocation motion yields [17]:

$$V_{eff} = kT\frac{ln(\dot{\tau}_{i2}/\dot{\tau}_{i1})}{\Delta\tau} \tag{2}$$

where the numerator and denominator in the parentheses correspond to the stress rate at the onset of relaxation 2 and at the finish of stress relaxation 1, respectively. The quotient of the mobile dislocation density at a time $\rho_{m(t)}$ and the mobile dislocation density at the onset of repeat relaxation $\rho_{m(0)}$ yields:

$$\frac{\rho_{m(ij)}}{\rho_{m(0)}} = \frac{\dot{\tau}_{ij}}{\dot{\tau}_{i1}}(j = 1, 2, 3...) \tag{3}$$

The total density of states (DOS) at Fermi level for Fe_{16} is 15.16 states/Ry atom (theoretical value: 15.37 [18]), and for Fe_{15} is 15.64 states/Ry atom. The DOS at the Fermi level in the H-containing BCC iron is found to be reduced. This is different from FCC iron with H occupied at octahedral site, in which the DOS increases as reported by Gavriljuk's group [4].

As shown in Fig. 1, there is a strong peak for projected DOS (PDOS) at -8.62 eV ($E - E_F$) on the nearest neighbor Fe atom of interstitial H (Fe_{nn}). The -8.62 eV peaks in all Fe orbitals correspond to the H-1s states which indicate strong bonding interaction between Fe and H.

The total charge of H, individual iron atom (with no neighbor H atoms, Fe_{in}) and the Fe_{nn} atom resulted from the Bader analysis are shown in Table 1. The total charge of Fe_{in} remains the same as in the hydrogen free bulk. Charge variation of $+0.40e^-$ occurs on the H atom, and $-0.07e^-$ occurs on

the nearest neighbor Fe atom. It has been reported that charge transference of -0.31e$^-$ appears from Fe_{nn} atom near an edge dislocation of BCC iron [19].

With a grid refinement number of 4, the distributions of all-electron density (in a unit of Bohr^{-3}) for Fe_{nn}, H and vacancy are calculated and characterized by plotting contour surfaces with different isovalues in Fig. 2. Fe_{nn} atom expresses bonding behavior with H atom in Fig. 2a, and the distance of Fe_{nn}-H bond is less than the Fe_{nn}-Fe_{in} bond as shown in Table 1. Hydrogen atoms increase the electron charges in tetrahedral sites of the bulk (Fig. 2b) and also in the vacancy (Fig. 2c and Fig. 2d).

Although the H-induced variations in DOS at Fermi level for BCC iron are in opposite tendency with FCC iron, the result that hydrogen decreases electron density of Fe atom is in accordance with the FCC iron system [4]. Unlike the carbon atom enhances local electron density of iron atoms and assists the covalent character of inter-atomic bonds [20], hydrogen increases the concentration of electrons in lattice and promotes the metallic character of atom interactions. Compared with covalent bonds, the metallic character could increase the local plasticity of metal and the mobility of dislocations.

After relaxation via DFT calculations, H atoms are stable in the tetrahedral sites of the lattice. The atomic forces in three axis for both H and Fe atoms are lower than 0.008 eV/Å. The strain field of an interstitial atom is calculated from the displacement of Fe_{nn} atoms after relaxation, $\epsilon_{ii} = (L_i - a)/a$, where L_i is length in the i axis of one cell after introducing H. By our DFT method, the strain tensor of C in octahedral sites of iron is calculated to be $\{\epsilon_{11}, \epsilon_{22}, \epsilon_{33}\} = \{0.21, -0.018, -0.018\}$, which is comparable to experiment value $\{0.38, -0.026, -0.026\}$ used in Cochardt's

calculation [5]. The strain field of one H atom in $Fe_{16}H_1$ is calculated to be $\{0.014, 0.041, 0.041\}$. The MD calculation in large scale results of $\{0.015, 0.059, 0.059\}$, and shows good agreement with the DFT calculation. The three components were considered to be identically equaled in none-DFT calculations for supporting HELP theory [2, 21]. However, using the same parameter as BCC calculation in a FCC (2×2×2) cell ($Fe_{32}H_1$) the strain tensor of H atom at octahedral site is calculated to be $\{0.0327, 0.0327, 0.0327\}$, which is isotropic.

Following the Cochardt's model, the interaction energy of hydrogen atoms at position $r = b$ and an edge dislocation laying in $< 211 >$ with b in the direction $< \bar{1}11 >$ is calculated. Since H atom may cause the less dilatation of 0.014 along axes 1, 2 or 3, there are three sets of constant in Eq. (1). The interaction energies are plotted in Fig. 3a, where angle ψ is the angle between $< \bar{1}11 >$ and the radius vector from the dislocation to the considered elementary cell. It is shown that the lowest interaction energy locates at $\psi = 270$ degrees, and thus H atoms prefer to stay below the extra half plane of edge dislocations. The lowest energy comes from H atom with strain field of $\{0.014, 0.041, 0.041\}$, and the minimum $U^E_{DH} = -0.24$ eV.

The interaction for a screw dislocation in [111]-direction and H atoms at position $r = b$ is calculated and shown in Fig. 3b, where φ is angle between $[2\bar{1}\bar{1}]$-axis and the normal direction of plane containing $\mathbf{r}$ and $\mathbf{b}$. Because of the trigonal symmetry of $< 111 >$ axis, there is a phase difference of ±120 degrees for H atom in different positions. The angular dependence of U^S_{DH} characterized in Fig.3b indicates that there are three equivalent positions of lowest energy at $\varphi = 0, 120$ and 240 degrees with minimum $U^S_{DH} = -0.051$

eV.

The interactions of H with edge dislocation and screw dislocation have been calculated in considerable quantity of DFT and MD calculations, and most of the works agree that hydrogen can be trapped by both edge and screw dislocation cores [15, 22]. However, the trap energy reported in those works are strongly depending on the position of H atom which is hard to be predicted during energy minimization, and the trapping behavior of screw dislocation is generally considered to be the influence of core structure[23]. The method used in this study shows the elastic energy and position relationship for both edge and screw dislocation. Due to the elastic interaction, it indicates that H atom can be trapped by screw dislocation even away from the dislocation core area.

During plastic deformation, the cross slip of perfect screw dislocation is more important than the behavior of edge dislocations, for the unrecoverable jogs it forms. As the group of Chateau pointed out [21], hydrogen atom influence the cross slip of perfect screw dislocation in FCC mainly by screening interaction of two edge partials, but this theory can not be applied to BCC metal directly due to there is no partial dislocations. By comparing the accumulation of H around a screw and an edge dislocation, one can find that the segregation of H atom takes place only below the glide plane of an edge dislocation but all around a screw dislocation, roughly the screw can bind twice as many H atoms as an edge dislocation. Although the elastic interaction energy away from the screw dislocation core is much less than the case of edge dislocation, increase of local H concentration could magnify the H-screw interactions and influence the mechanical property of BCC metals.

As shown in Fig. 4a, at low cathodic current density, the yield stress increases 5 MPa at most and the effective activation volume is almost constant, which indicates dislocation motion is impeded when the H concentration is low. As the interaction energy for H-edge is almost 5 times more than H-screw interaction, at low H concentration the H-edge interaction could be stronger than the H-screw one. Moreover, the hydrogen shielding in this case may have less effect on enhancing dislocation mobility, as the flow stress increases during tensile test, the deformation process is possibly controlled by the H solute drag effect.

The mobile dislocation density decreases rapidly in hydrogen-free iron after even one cycle in Fig. 4b. At higher H concentration, the dislocation density decreases with a slower speed, and it can still maintain at a stable value after 5 cycles. This and the steep decrease of effective activation volume in Fig. 4a together signify that hydrogen could increase the mobility of dislocations in BCC iron at higher cathodic current densities more than 25 mA/cm^2. The elastic interactions of H-edge and H-screw dislocation is proportional to the H concentration. At high H concentrations, the screw dislocation is able to trap more hydrogen atoms than the edge one and the interaction of H and screw dislocation is much more important in this condition. The enhanced cross slip and jog formation caused by H shielding effect as reported by Chateau et. al [21] could be the main reason for the steep reduction of yield stress and effective activation volume after 25 mA/cm^2.

In summary, H in BCC iron can increase the electron densities at tetrahedral sites and vacancy, and that the hydrogen-enhanced metallic character of inter-atomic bonds can increase the mobility of dislocations and contribute

to the HELP theory. Two components of strain tensor for H interstitial atom are calculated to be unequal, which is expected to cause elastic interaction of H with screw dislocations, as it does with edge dislocations. For the angular dependence of H-edge dislocations interaction, H atoms prefer to stay under extra atomic plane, while for screw dislocation there are more positions for the lowest interaction energy and high local H concentration is possible. The repeated transients tests for H-charged α-iron indicate that significant hydrogen enhanced plasticity can be observed with relative high H concentrations, and in those cases, the H-screw interaction should be considered, and it is possible to lead for a new understanding of hydrogen embrittlement in BCC iron.

Acknowledgments

This work is suppoted in part by Hokkaido university academic cloud, information initiative center. We wish to thank Prof. S. Miura at Laboratory of Materials Modeling, Hokkaido University, for enlightening discussions and advices.

[1] J. Hirth, Metallurgical and Materials Transactions A 11 (1980) 861–890.

[2] H. K. Birnbaum, P. Sofronis, Materials Science and Engineering: A 176 (1994) 191–202.

[3] K. Takita, K. Sakamoto, Scripta Metallurgica 10 (1976) 399 – 403.

[4] V. Gavriljuk, V. Shivanyuk, B. Shanina, Acta Materialia 53 (2005) 5017–5024.

[5] A. Cochardt, G. Schoek, H. Wiedersich, Acta Metallurgica 3 (1955) 533–537.

[6] J. J. Mortensen, L. B. Hansen, K. W. Jacobsen, Physics Review: B 71 (2005) 035109.

[7] P. E. Blöchl, Physical Review B (1994).

[8] S. R. Bahn, K. W. Jacobsen, COMPUTING IN SCIENCE & ENGINEERING 4 (2002) 56–66.

[9] J. P. Perdew, K. Burke, M. Ernzerhof, Physics Review Letter 77 (1996) 3865–3868.

[10] H. J. Monkhorst, J. D. Pack, Physics Review: B 13 (1976) 5188–5192.

[11] J. D. Pack, H. J. Monkhorst, Physics Review: B 16 (1977) 1748–1749.

[12] W. Tang, E. Sanville, G. Henkelman, Journal of Physics: Condensed Matter 21 (2009) 084204.

[13] R. F. W. Bader, Atoms in Molecules: A Quantum Theory, Oxford University Press, 1990.

[14] V. Cocula, C. Pickard, E. Carter, Journal of Chemical Physics 123 (2005).

[15] A. Ramasubramaniam, M. Itakura, E. A. Carter, Physical Review B (2009).

[16] S. Plimpton, Journal of Computational Physics 117 (1995) 1 – 19.

[17] P. Spatig, J. Bonneville, J. L. Martin, Materials Science and Engineering: A 167 (1993) 73–79.

[18] J. Callaway, C. S. Wang, Physics Revive: B 16 (1977) 2095–2105.

[19] M. Pronsato, G. Brizuela, A. Juan, Applied Surface Science 173 (2001) 368 – 379.

[20] S. M. Teus, V. N. Shivanyuk, B. D. Shanina, V. G. Gavriljuk, physica status solidi (a) 204 (2007) 4249–4258.

[21] J. P. Chateau, D. Delafosse, T. Magnin, Acta Materialia 50 (2002) 1507–1522.

[22] B. J. Lee, J. W. Jang, Acta Materialia 55 (2007) 6779–6788.

[23] M. Wen, X. J. Xu, S. Fukuyama, Journal of Materials ... (2001).

Figure Captions

1. Fig. 1 Projected density of states over iron and H atoms.
2. Fig. 2 Contour surfaces of electron density in Fe-H system by Bader analysis. (a) Fe_{nn} atom, with isovalue of 0.08 $Bohr^{-3}$. (b) Interstitial H atom at tetrahedral site of iron lattice, with isovalue of 0.08 $Bohr^{-3}$. (c) Hydrogen-free vacancy, with isovalue of 0.02 $Bohr^{-3}$. (d) Vacancy binding with H atom, with isovalue of 0.02 $Bohr^{-3}$.
3. Fig. 3 Elastic interactions of Hydrogen and different kinds of dislocation. (a) Edge dislocation laying in$< 211 >$, b=$< \bar{1}11 >$. (b) Screw dislocation in [111]-direction.
4. Fig. 4 Thermal activation analysis of dislocation motion in hydrogen charged BCC iron. (a) Variation of effective activation volume (left axis) and yield stress (right axis) at different H concentrations. (b) Evolution of mobile dislocation density with and without H.

Table Captions

1. Table 1 Variation of charges and bonding behavior in BCC iron containing H.

Table 1: Variation of charges and bonding behavior in BCC iron containing H.

Atom	Bader charge	Bond	Distance (Å)
Fe_{in}	25.9437	Fe_{in}-Fe_{nn}	2.392
Fe_{nn}	25.8713	Fe_{nn}-H	1.681
H	1.4024		

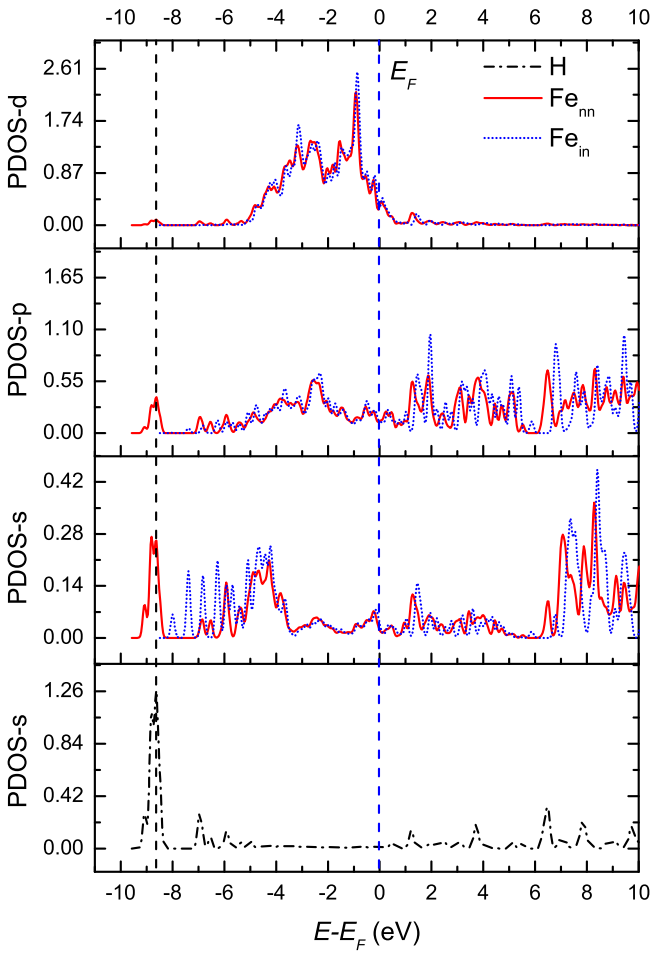

Figure 1: Projected density of states over iron and H atoms.

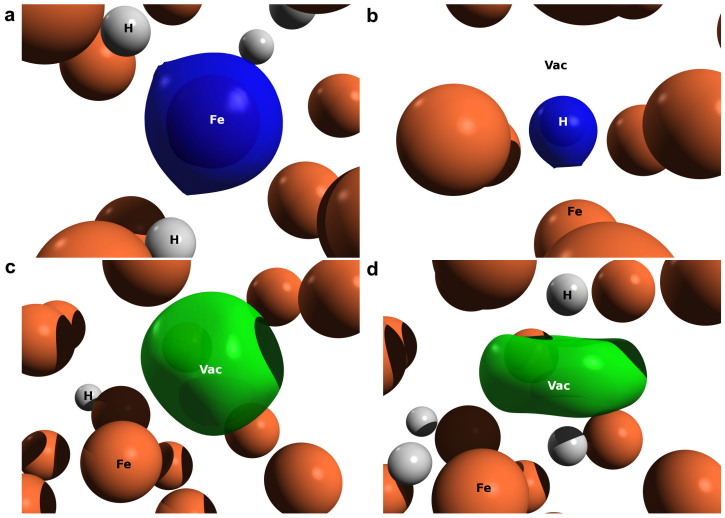

Figure 2: Contour surfaces of electron density in Fe-H system by Bader analysis. (a) Fe_{nn} atom, with isovalue of 0.08 $Bohr^{-3}$. (b) Interstitial H atom at tetrahedral site of iron lattice, with isovalue of 0.08 $Bohr^{-3}$. (c) Hydrogen-free vacancy, with isovalue of 0.02 $Bohr^{-3}$. (d) Vacancy binding with H atom, with isovalue of 0.02 $Bohr^{-3}$.

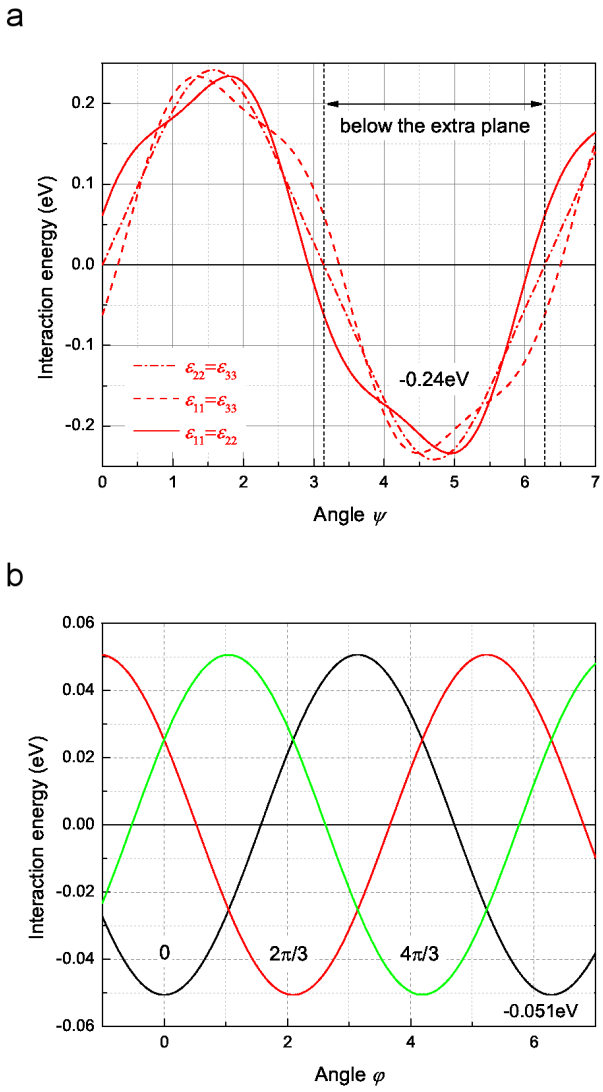

Figure 3: Elastic interactions of Hydrogen and different kinds of dislocation. (a) Edge dislocation laying in$< 211 >$, b=$< \bar{1}11 >$. (b) Screw dislocation in [111]-direction.

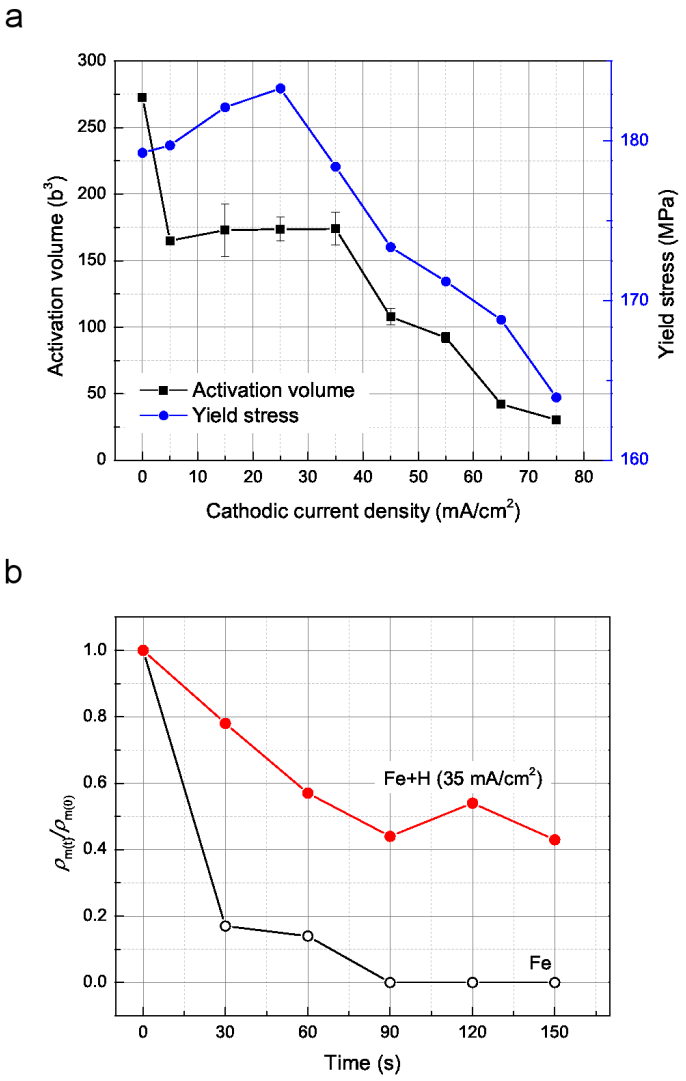

Figure 4: Thermal activation analysis of dislocation motion in hydrogen charged BCC iron. (a) Variation of effective activation volume (left axis) and yield stress (right axis) at different H concentrations. (b) Evolution of mobile dislocation density with and without H.